

Optimization of Variance Reduction Techniques used in EGSnrc Monte Carlo Codes

Sangeetha Shanmugasundaram, Sureka Chandrasekaran¹

Departments of Physics and ¹Medical Physics, Bharathiar University, Coimbatore, Tamil Nadu, India

Abstract

Monte Carlo (MC) simulations are often used in calculations of radiation transport to enable accurate prediction of radiation-dose, even though the computation is relatively time-consuming. In a typical MC simulation, significant computation time is allocated to following non-important events. To address this issue, variance reduction techniques (VRTs) have been suggested for reducing the statistical variance for the same computation time. Among the available MC simulation codes, electron gamma shower (National Research Council of Canada) (EGSnrc) is a general-purpose coupled electron-photon transport code that also features an even-handed, rich set of VRTs. The most well-known VRTs are the photon splitting, Russian roulette (RR), and photon cross-section enhancement (XCSE) techniques. The objective of this work was to determine the optimal combination of VRTs that increases the simulation speed and the efficiency of simulation, without compromising its accuracy. Selection of VRTs was performed using EGSnrc MC User codes, such as cavity and egs_chamber, for simulating various ion chamber geometries using 6 MV photon beams and 1.25 MeV ⁶⁰Co photon beams. The results show that the combination of XCSE and RR yields the highest efficiency for ion-chamber dose calculations inside a 30 cm × 30 cm × 30 cm water phantom. Hence, properly selecting a different VRT without altering the underlying physics increases the efficiency of MC simulations for ion-chamber dose calculation.

Keywords: EGSnrc Monte Carlo Code, Ionization Chamber, Monte Carlo Simulation, variance reduction techniques

Received on: 26-10-2017

Review completed on: 05-06-2018

Accepted on: 14-06-2018

INTRODUCTION

Significant technological progress and increased understanding of radiation phenomena and their consequences on living cells secured radiation therapy as a critical tool for cancer treatment. In light of this, modern radiotherapy practitioners seek to increase precision in dose calculation. Among many algorithms formulated recently for evaluating dose distributions, Monte Carlo (MC)-based methods have proven to be extremely promising regarding accuracy, by furnishing outcomes that are more realistic without biasing the results.^[1,2] In the field of teletherapy, MC simulations are often used in the calculations of radiation transport to enable accurate prediction of radiation-dose. However, by definition, a typical MC simulation is relatively a time-consuming method in which significant time is allocated to following nonimportant events that prevent their usage in teletherapy.

Although MC methods yield more accurate results compared with other methods, using these methods in practice remains challenging, mainly owing to a significant computing

time required to achieve an acceptable level of statistical uncertainty.^[3]

To address this issue, variance reduction techniques (VRTs) have been suggested, to reduce the simulation time and uncertainties and to improve the statistical results for the same computation time.^[4] However, for obtaining good statistical outcomes and consistent responses in short time, VRTs should be used properly. Hence, almost all MC codes offer several VRTs. Wulff *et al.*^[5] implemented several VRTs using a couple of EGSnrc MC User codes (cavity and egs_chamber). These techniques dramatically improve the simulation efficiency of NE2571 Farmer-type ion-chamber dose and perturbation factor calculations. These authors concluded that combining different VRTs could be useful for situations that involve the

Address for correspondence: Dr. Sureka Chandrasekaran,
Department of Medical Physics, Bharathiar University,
Coimbatore - 641 046, Tamil Nadu, India.
E-mail: surekasekaran@buc.edu.in

This is an open access journal, and articles are distributed under the terms of the Creative Commons Attribution-NonCommercial-ShareAlike 4.0 License, which allows others to remix, tweak, and build upon the work non-commercially, as long as appropriate credit is given and the new creations are licensed under the identical terms.

For reprints contact: reprints@medknow.com

How to cite this article: Shanmugasundaram S, Chandrasekaran S. Optimization of variance reduction techniques used in EGSnrc Monte Carlo Codes. *J Med Phys* 2018;43:185-94.

Access this article online

Quick Response Code:



Website:
www.jmp.org.in

DOI:
10.4103/jmp.JMP_132_17

computation of dose in a relatively small volume and not just for ion-chamber-related calculations.

In this work, we examined several combinations of VRTs to determine which set of VRTs is preferable for ion-chamber-related dose calculations. The objective of this chapter was to determine the optimal combination of VRTs that increases the simulation speed and the efficiency of simulation, without compromising its accuracy. Selection of VRTs was performed for EGSnrc MC User codes, such as cavity and `egs_chamber`, for simulating various ion chamber geometries using 6 MV photon beams. The dose calculations have been performed for various combinations of VRTs only within the user-defined treatment field, employing the EGSnrc MC codes, which offers a library of VRTs. Detailed descriptions of all the VRTs implemented in this work, have been benchmarked by comparing the BEAMnrc MC simulations with and without VRTs. After the evaluation of VRTs, the appropriate optimized technique has been utilized to validate the modeled linear accelerator using BEAMnrc MC code. From this study, it is concluded that an appropriate selection of VRTs without altering the underlying physics increases the efficiency of MC simulations for ion-chamber dose calculations.

MATERIALS AND METHODS

Monte Carlo simulation

MC simulations are often referred to as stochastic simulations, which allow everyone to access all the credible consequences of facts and to appraise the impact of ventures, yielding preferable options for decision-making under precarious conditions. From the computational perspective, stochastic MC simulations are sturdy and sublimely efficient. Thus, MC methods have been used extensively in complex problems because they provide reasonable approximations with higher accuracy compared with other techniques. In radiation therapy, MC methods are used for simulating the radiation transport, to deliver a precise and accurate dose to a target.^[1]

In MC simulations, the transport of photons and electrons is modeled by recording the history of each particle's interactions, until that particle reaches predetermined threshold energy, electron and photon cutoff energies and condensed history step sizes.^[2] MC simulations have been widely used in various branches of radiation medicine, particularly in the areas of radiation dosimetry, radiation shielding, teletherapy treatment planning, and radiological imaging.^[6-8] In the last few decades, the use of MC methods in medical radiation physics has increased dramatically, owing both to the availability of general-purpose MC codes (EGSnrc, GEANT4, MCNP, PENELOPE, ETRAN, ITS) and to the ever-increasing computation speed and reduction in the cost of data processing.^[9]

In this present work, we have chosen the EGSnrc MC code (EGS4 Version) developed at the Los Alamos National Laboratory^[10,11] because it is a general-purpose package for MC simulations of the coupled electron-photon transport in an arbitrary geometry involving a dynamic range of particle

energies, from 1 keV to several hundreds of Gigaelectronvolt.^[12] Our ultimate motivation for using the EGSnrc MC code is the fact that most of the MC systems in teletherapy either entirely or partially utilize this code. All of the simulations in the present study were one of the following: using EGSnrc MC User codes such as cavity and `egs_chamber` and further validated with BEAMnrc MC Simulation code.

1. Simulations with VRTs
2. Simulations without VRTs and using EGSnrc MC user code such as cavity and `egs_chamber`.

In the second set of simulations, several combinations of VRTs, namely PS, RR, and photon cross-section enhancement (XCSE) were considered, to investigate which VRT is preferable for calculating the ion-chamber dose and for enhancing the efficiency of the calculation. The results, described below, were obtained by averaging over 10^6 particle histories traces. In these simulations, we used 6 MV photon beams for Farmer-type (NE2571 and N30013) ionization chambers and 1.25 MeV ⁶⁰Co photon beams for cylindrical type (National research council (NRC), and pancake) ionization chambers within a 30 cm × 30 cm × 30 cm homogeneous water phantom. In all simulations, the default MC transport parameters were AE = electron transport cutoff (ECUT) = 0.521 MeV and AP = photon transport cutoff (PCUT) = 0.01 MeV. In a final simulation setup, we investigated the beam characteristics for a Varian linac machine “Varian Clinac 600 C/D” with a VRT-optimized ion chamber. The calculations were performed on a Kernel Linux 2.6.35.6-45.fc14.1686 workstation with a 100 GB memory, with an Intel Xenon E5606 computation (CPU) running at 2.13 GHz.

Construction of ionization chambers

In general, an ionization chamber is the most practical and broadly used type of dosimeter for accurately measuring machine output in radiotherapy.^[13] Hence, in the present work, we have considered different types of ionization chambers to examine the consequences of cavity dose calculations using various combinations of VRTs, for a broad range of geometric shapes. We modeled various types of ionization chamber geometries such as cylindrical, parallel-plate, and Farmer-type chambers, using the `egspp C++` class library from the EGSnrc MC Code system.^[14] The geometry specifications of the parallel-plate (pancake chamber) and Farmer-type chambers (NE2571 and N30013 models) were obtained from the manufacturers, whereas a detailed description of cylindrical ion chamber geometry (NRC's 3C model) was obtained from Canada's primary standard for air kerma in a ⁶⁰Co beam.^[15] The physical characteristics of the EGSnrc-modeled various types of ionization chamber geometries are elaborately listed in Table 1.

Efficiency of Monte Carlo simulations

The efficiency ε of an MC simulation can be computed using the figure of merit defined by the MCNPX code developers according to Equation (1).^[16-20]

$$\varepsilon = \frac{1}{\sigma^2 T} \quad (1)$$

where T is the CPU time needed for the overall simulation and σ is the statistical uncertainty of the quantity of interest (i.e., the cavity dose in the present simulation). In general, the efficiency of MC simulations can be increased in one of the two ways:

1. Reducing the variance
2. Reducing the CPU time per simulated particle.

Variance reduction techniques

In any MC code, VRTs play an important role in reducing uncertainties and increasing the precision of the statistical results. The implementation of different VRTs in EGSnrc MC User codes, such as cavity and `egs_chamber` codes, is described briefly in what follows. The cavity user code allows calculating cavity doses for any ion chamber geometry.^[21] This code includes two powerful VRTs, namely photon splitting (PS) and Russian roulette (RR). The `egs_chamber` user code is an advanced EGSnrc application derived from the cavity user code. It allows calculating doses to the cavity of an ion chamber and dose ratios of two correlated geometries, as well as the perturbation factors which is defined as a correction factor accounting for perturbations caused by the chamber inserted into the medium. XCSE is a powerful VRT available in the `egs_chamber` code. In what follows, we briefly discuss the basic concepts of the above-mentioned VRTs and their impact on the simulation efficiency. A more technical description of these VRTs can be found elsewhere^[5,12,14,20] Along with the above-mentioned VRTs, additional EGSnrc transport parameters, namely ECUT, PCUT, and ESAVE have also been used for reducing the simulation time. The values of

ECUT and ESAVE were 0.521 MeV, and the value of PCUT was 0.01 MeV, within the encompassed treatment field, as has been documented recently.^[17,21,22] The detailed explanation of all the above mentioned VRTs^[23-25] are distinctly portrayed in the previous section of Materials and Methods.

RESULTS AND DISCUSSION

Optimization of particle histories

To optimize the particle histories, several test calculations were performed for particles, ranging from 1×10^4 histories to 1×10^9 histories. Table 2 lists the optimization parameters of particle histories for ion-chamber cavity dose calculations for various ion chambers. The simulation type, the relative statistical uncertainty σ , the efficiency ϵ , and the number of histories N are presented in Table 2. From Table 2, the cavity doses obtained in the simulations without VRTs are stable and range from 1×10^6 to 1×10^9 histories, for all cases. It is also observed that no improvement in the efficiency of the simulation has been achieved by further increasing the number of particle histories. However, increasing the number of particle histories effectively decreases the statistical uncertainty of the cavity dose, from $\pm 31.035\%$ to $\pm 0.176\%$ for the NRC 3C cylindrical ion chamber, from $\pm 18.505\%$ to $\pm 0.192\%$ for the parallel-plate pancake ion chamber, and from $\pm 3.962\%$ to $\pm 0.11\%$ and from $\pm 1.684\%$ to $\pm 0.553\%$ for the NE2571 and N30013 modeled Farmer-type ion chambers, respectively, without degrading the accuracy of the calculations.

Table 1: Physical characteristics of the EGSnrc modeled various types of ionization chamber geometries

Chamber specifications	Ionization chambers				
	NRC ion chamber (cylindrical)	Pancake ion chamber (parallel-plate)	Farmer type ion chamber		
			NE2571	N30013	
Sensitive volume (cm ³)	1.9	0.8	0.678	0.601	
Cavity length (cm)	2.5255	3.2	2.476	2.36	
Cavity radius (cm)	1.175	1.3	0.358	0.305	
Wall material	C	C	Air + C	PMMA + C	
Central electrode material	Air	Air	Al	Al	
Wall thickness (mm)	1.5102	1.3	0.408	0.36	

NRC: National research council

Table 2: Optimization of particles' histories for various ion-chamber geometries

Type of simulation	"N" histories	NRC 3C ion chamber (cylindrical)			Pancake ion chamber (parallel-plate)			Farmer type ion chamber					
								NE2571			N30013		
		Cavity dose (Gy)	σ	ϵ	Cavity dose (Gy)	σ	ϵ	Cavity dose (Gy)	σ	ϵ	Cavity dose (Gy)	σ	ϵ
Without VRT	1.10^4	1.41e-12	± 31.035	12	4.59e-12	± 18.505	5	3.09e-08	± 3.962	76	3.12e-08	± 1.684	41
	1.10^5	1.32e-12	± 18.796	13	5.18e-12	± 9.639	7	3.12e-08	± 1.150	194	3.10e-08	± 1.533	317
	1.10^6	1.20e-12	± 5.651	18	5.28e-12	± 3.013	12	3.13e-08	± 0.363	222	3.10e-08	± 1.169	603
	1.10^7	1.23e-12	± 1.800	18	5.33e-12	± 0.924	12	3.10e-08	± 0.213	230	3.11e-08	± 1.053	659
	1.10^8	1.22e-12	± 0.558	18	5.35e-12	± 0.291	12	3.10e-08	± 0.136	233	3.11e-08	± 1.017	660
	1.10^9	1.21e-12	± 0.176	18	5.35e-12	± 0.192	12	3.10e-08	± 0.11	235	3.11e-08	± 0.553	661

VRT: Variance reduction technique, NRC: National research council

As in Table 2, similar levels of efficiency are obtained for histories in the 1×10^6 to 1×10^9 range, for all cases. Based on these results, the optimal number of particle histories is determined to be 1×10^6 , and this particular number has been taken into account in the remaining simulations.

Efficiency gain by the implementation of photon splitting

The PS technique in EGSnrc MC Code is found to be very useful for ion-chamber dose-related calculations.^[12] In this part of the work, the PS technique has been implemented to determine how efficiency is affected by enhancing the N_Split factor. Table 3 depicts the implementation of PS and the effects on computation, where the type of simulation, cavity dose, relative statistical uncertainty σ , and their respective efficiency ϵ are given. It summarizes the effect of PS techniques carried out in this work.

It is clearly observed that the relative uncertainty obtained in calculations is decreased up to 0.428% for NRC 3C cylindrical ion chamber, $\pm 0.19\%$ for parallel-plate pancake ion chamber, $\pm 0.33\%$ and $\pm 0.160\%$ for NE2571 and N30013 modeled Farmer-type ion chambers whereas the computation time is increased when the PS factor has been enhanced by 256. This is due to the fact that the primary aim of the PS technique is to increase the density of interactions throughout the entire simulation geometry. Hence, it implicates a wide fraction of the overall geometry; the computation time will be reduced by default. It is also noted that the improvement in efficiency is not achieved by further enhancing the PS factor beyond 16 for all cases. This implies that the splitting number should not be set too high in the geometry since it introduces correlations, which may not be desirable. It reveals that an appropriate selection of the PS number defined by the user plays a vital role in achieving the best efficiency. Thus, we have determined that 16 is the optimal PS factor to be used for further simulation work.

Consequently, we concluded that the simulation involving the proper usage of PS technique improves the efficiency by

a factor of 23 for NRC 3C cylindrical ion chamber, 17.5 for parallel-plate pancake ion chamber, 234 and 684 for NE2571 and N30013-modeled Farmer-type ion chambers when compared to the simulation without using the VRT.

Efficiency gain by range-rejection-based Russian roulette

In this part of the work, the range-rejection-based RR technique has been implemented to carry out the objective. The advantage of implementing the effect of RR is evident in Table 4 where the type of simulation, quantity of interest (the cavity dose in the present simulation), relative statistical uncertainty σ , and the simulation efficiency ϵ are depicted.

In Table 4, it is observed that the statistical uncertainty σ obtained in the present simulation of implementing the range-rejection-based RR is slightly lower than that obtained in the present simulation without using the VRT. As seen in the agreement between both types of simulations in Table 4, a similar level of cavity dose is achieved effectively for all cases. At the same time, the simulation efficiency has been increased further, while enhancing the RR factor. The progressive technique of range-rejection-based RR terminates the low-energy electrons from reaching the ion-chamber cavity, which counteracts the electron to the chamber dose directly. This, in turn, leads to an increase in the statistical weight of the electrons often referred to as “fat electrons.” These fat electrons may generate high-weight photons, which result in large statistical fluctuations due to other types of nuclear interactions. Since the range-rejection-based RR is applied only to nonfat electrons, it avoids the approximation that arises by neglecting the feasible photons set in motion by the rejected electrons. Thus, computation time is not increased by following the nonrelevant events of fat electrons.

From Table 4, one may observe that further increasing the RR factor above 64 clearly reveals that when the range-rejection value is below the minimum level, the efficiency of the simulation decreases significantly. However, it is also noted

Table 3: Comparison of the efficiency for cavity-dose calculations by the implementation of photon splitting technique using EGSnrc Monte Carlo user code for various ion chamber geometries

Type of simulation	NRC 3C ion chamber (cylindrical)				Pancake ion chamber (parallel-plate)				Farmer type ion chamber								
									NE2571				N30013				
	Cavity dose (Gy)	σ	ϵ	CPU time (s)	Cavity dose (Gy)	σ	ϵ	CPU time (s)	Cavity dose (Gy)	σ	ϵ	CPU time (s)	Cavity dose (Gy)	σ	ϵ	CPU time (s)	
PS factor																	
-	1.20e-12	± 5.65	18	6.3	5.33e-12	± 3.01	12	35.2	3.10e-08	± 0.36	222	121	3.11e-08	± 0.169	603	210	
2	1.16e-12	± 3.89	20	10.9	5.32e-12	± 1.97	15.5	59.3	3.10e-08	± 0.35	228	120.9	3.109e-08	± 0.165	680	188.4	
4	1.24e-12	± 2.88	21	20.7	5.36e-12	± 1.42	15.9	111.1	3.09e-08	± 0.34	233	121.5	3.109e-08	± 0.164	678	189.0	
8	1.23e-12	± 1.97	22	40.1	5.35e-12	± 1.01	16.4	214.9	3.10e-08	± 0.34	227	120.2	3.110e-08	± 0.164	678	188.9	
16	1.22e-12	± 1.40	23	79.2	5.35e-12	± 0.69	17.5	421.4	3.10e-08	± 0.34	234	120.5	3.109e-08	± 0.163	684	188.4	
32	1.22e-12	± 0.99	22	156.5	5.33e-12	± 0.50	17.1	834.2	3.10e-08	± 0.34	233	121	3.110e-08	± 0.162	682	187.8	
64	1.22e-12	± 0.74	22	311.5	5.34e-12	± 0.35	17.2	1652	3.10e-08	± 0.34	233	121	3.111e-08	± 0.162	679	189.7	
128	1.21e-12	± 0.55	19	617.0	5.33e-12	± 0.26	15.4	3274	3.10e-08	± 0.33	232	120.9	3.110e-08	± 0.161	675	188.6	
256	1.24e-12	± 0.42	11	1234	5.34e-12	± 0.19	14.2	6692	3.10e-08	± 0.33	218	121.2	3.110e-08	± 0.160	672	188.7	

PS: Photon splitting, CPU: Computation, NRC: National research council

that the use of range-rejection-based RR significantly reduces the statistical error from $\pm 5.651\%$ to $\pm 4.99\%$ for NRC 3C cylindrical ion chamber, $\pm 3.01\%$ to $\pm 2.91\%$ for parallel-plate pancake ion chamber, $\pm 0.36\%$ to $\pm 0.31\%$ and $\pm 0.17\%$ to $\pm 0.16\%$ for NE2571 and N30013-modeled Farmer-type ion chambers, respectively without degrading the accuracy of the calculations along with the increase in the efficiency by as much as a factor of 56 for NRC 3C cylindrical ion chamber, 26 for parallel-plate pancake ion chamber, 397 and 791 for NE2571 and N30013-modeled Farmer-type ion chambers when compared to the simulation without using the VRT.

Efficiency gain by the combination of photon splitting and Russian roulette

To evaluate the efficiency of the simulation effectively, we adopted the method of PS and investigated the effect of

range-rejection-based RR to study our objective. The feasible results of the standardized methodology of the VRT described above are depicted in Table 5, where the type of simulation, quantity of interest (i.e., the cavity dose), relative statistical uncertainty σ , and simulation efficiency ϵ are sketched. Table 5 summarizes the effect of implementing the combination of PS and range-rejection-based RR using EGSnrc MC cavity user code. It shows that the similar levels of cavity doses are obtained even when enhancing the values of ESAVE (a parameter available in BEAMnrc which allows the user to select the threshold energy of the electron). The level of statistical error has been reduced to $\pm 0.43\%$ from the error of $\pm 5.651\%$ for NRC 3C cylindrical ion chamber, $\pm 3.01\%$ to $\pm 0.70\%$ for parallel-plate pancake ion chamber, and it remains same for NE2571 and N30013-modeled Farmer-type ion chambers.

Table 4: Comparison of the efficiency for cavity-dose calculations by the implementation of Russian roulette technique using EGSnrc Monte Carlo user code for various ion chamber geometries

Type of simulation	NRC 3C ion chamber (cylindrical)				Pancake ion chamber (parallel-plate)				Farmer-type ion chamber							
									NE2571				N30013			
	Cavity dose (Gy)	σ	ϵ	CPU time (s)	Cavity dose (Gy)	σ	ϵ	CPU time (s)	Cavity dose (Gy)	σ	ϵ	CPU time (s)	Cavity dose (Gy)	σ	ϵ	CPU time (s)
PS factor																
-	1.20e-12	± 5.65	18	6.3	5.33e-12	± 3.01	12	35.2	3.10e-08	± 0.36	222	121	3.11e-08	± 0.169	603	210
2	1.16e-12	± 3.89	20	10.9	5.32e-12	± 1.97	15.5	59.3	3.10e-08	± 0.35	228	120.9	3.109e-08	± 0.165	680	188.4
4	1.24e-12	± 2.88	21	20.7	5.36e-12	± 1.42	15.9	111.1	3.09e-08	± 0.34	233	121.5	3.109e-08	± 0.164	678	189.0
8	1.23e-12	± 1.97	22	40.1	5.35e-12	± 1.01	16.4	214.9	3.10e-08	± 0.34	227	120.2	3.110e-08	± 0.164	678	188.9
16	1.22e-12	± 1.40	23	79.2	5.35e-12	± 0.69	17.5	421.4	3.10e-08	± 0.34	234	120.5	3.109e-08	± 0.163	684	188.4
32	1.22e-12	± 0.99	22	156.5	5.33e-12	± 0.50	17.1	834.2	3.10e-08	± 0.34	233	121	3.110e-08	± 0.162	682	187.8
64	1.22e-12	± 0.74	22	311.5	5.34e-12	± 0.35	17.2	1652	3.10e-08	± 0.34	233	121	3.111e-08	± 0.162	679	189.7
128	1.21e-12	± 0.55	19	617.0	5.33e-12	± 0.26	15.4	3274	3.10e-08	± 0.33	232	120.9	3.110e-08	± 0.161	675	188.6
256	1.24e-12	± 0.42	11	1234	5.34e-12	± 0.19	14.2	6692	3.10e-08	± 0.33	218	121.2	3.110e-08	± 0.160	672	188.7

PS: Photon splitting, CPU: Computation, NRC: National research council

Table 5: Comparison of the efficiency for cavity-dose calculations by the implementation of photon splitting + Russian roulette technique using EGSnrc Monte Carlo user code for various ion chamber geometries

Type of simulation	NRC 3C ion chamber (cylindrical)				Pancake ion chamber (parallel-plate)				Farmer type ion chamber							
									NE2571				N30013			
	Cavity dose (Gy)	σ	ϵ	CPU time (s)	Cavity dose (Gy)	σ	ϵ	CPU time (s)	Cavity dose (Gy)	σ	ϵ	CPU time (s)	Cavity dose (Gy)	σ	ϵ	CPU time (s)
PS + RR factor																
-	1.20e-12	± 5.65	18	6.3	5.33e-12	± 3.01	12	35.2	3.10e-08	± 0.36	222	121	3.11e-08	± 0.169	603	210
2	1.21e-12	± 3.98	61	3.7	5.34e-12	± 0.71	24.2	288	3.10e-08	± 0.5	118	122	3.106e-08	± 0.17	797	160.8
4	1.31e-12	± 2.98	65	6.2	5.37e-12	± 0.72	33.2	208	3.11e-08	± 0.4	193	116	3.105e-08	± 0.17	780	158.2
8	1.20e-12	± 1.85	83	11.1	5.35e-12	± 0.72	41.6	166	3.09e-08	± 0.4	197	114	3.110e-08	± 0.17	787	156.8
16	1.20e-12	± 1.37	94	20.9	5.33e-12	± 0.66	56.2	145	3.11e-08	± 0.31	318	113	3.110e-08	± 0.16	852	156.2
32	1.21e-12	± 0.99	89	40.6	5.34e-12	± 0.72	51.2	135	3.08e-08	± 0.37	223	112	3.110e-08	± 0.17	728	157.5
64	1.22e-12	± 0.72	85	79.2	5.33e-12	± 0.72	53.7	129	3.08e-08	± 0.53	112	112	3.111e-08	± 0.18	639	156.4
128	1.20e-12	± 0.54	76	156.6	5.33e-12	± 0.71	55.1	127	3.07e-08	± 0.79	51.8	111	3.108e-08	± 0.20	529	156.0
256	1.21e-12	± 0.43	62	310.4	5.33e-12	± 0.70	55.0	130	3.13e-08	± 1.23	21.1	112	3.109e-08	± 0.22	458	155.8

RR: Russian roulette, CPU: Computation, PS: Photon splitting, NRC: National research council

Consequently, the simulation efficiency has improved significantly by a factor >94 for NRC 3C cylindrical ion chamber, 56 for parallel-plate pancake ion chamber, 318 and 852 for NE2571 and N30013-modeled Farmer-type ion chambers when compared to the simulation without using the VRT. The PS technique generally increases the particle’s weight whereas the implementation of RR decreases the particle’s weight. Sections of “efficiency gain by the implementation of PS,” and “efficiency gain by range rejection-based RR,” reveal the fact that the dispersion in particle weight will considerably degrade the efficiency of the simulation.

Hence, we implemented a proper combination of these two methods to yield relatively small dispersion of particles by focusing mainly on reducing the variance. This is achieved by subjecting all of the electrons with polar angles above a selected ESAVE to RR so that their descendant photons are split. This results in the immediate termination of most electrons through RR after they are set in motion in a split photon interaction. This termination improves the computation time by excluding the simulation of electrons that are not contributory to the cavity. Table 5 also reveals that while enhancing the ESAVE values, the efficiency of the simulation also is enhanced without affecting the physical results. However, while increasing the ESAVE values above 16, the efficiency is reduced since the value of range rejection below the minimum level decreases the efficiency of the simulation.

Efficiency gain by the implementation of photon cross-section enhancement

In the preceding four sections of this work, all of the calculations have been performed using EGSnrc MC cavity user code. In this section, however, the entire simulation has been carried out using EGSnrc MC egs_chamber user code. Table 6 depicts the effect of the implementation of XCSE where

the type of simulation, quantity of interest (i.e., the cavity dose), relative statistical uncertainty σ , and simulation efficiency ϵ are given. In Table 6, it is found that the cavity doses remain almost constant when one compares the cavity dose levels obtained using the simulation without the VRT. It is also noted that the relative statistical error is reduced from $\pm 5.65\%$ to $\pm 0.27\%$ for NRC 3C cylindrical ion chamber, $\pm 3.01\%$ to $\pm 0.1\%$ for parallel-plate pancake ion chamber, and $\pm 0.10\%$ to $\pm 0.02\%$ and $\pm 0.169\%$ to $\pm 0.03\%$ for NE2571 and N30013-modeled Farmer type ion chambers without affecting the accuracy of simulation.

Table 6 highlights the level of efficiency increases up to a factor of 52 for NRC 3C cylindrical ion chamber, 30 for parallel-plate pancake ion chamber, 371 and 699 for NE2571 and N30013-modeled Farmer-type ion chambers when compared to the simulation without using the VRT. This is due to the fact that the basic focus of XCSE is to increase the photon cross-section enhancement by a parameter $b > 1$ for the purpose of reducing the mean free path of the photons. This is the case because the mean free path of the photons in water will be significantly larger than the typical dimensions of the phantom, creating more fluctuations in the statistical weight of the particles. By decreasing the mean free path of the photons, it is possible to generate greater numbers of electrons along the path of a photon. However, these generated electrons may have different statistical weights, which lead to statistical fluctuations. To avoid these fluctuations, the electrons whose statistical weights have the ratio of the original weight to the XCSE factor of b alone are taken into account, which degrades the computation time. When further enhancing the XCSE factor to a value >128 , however, a consistent decrease in the efficiency level. Thus, in this part of the work, the optimized value of XCSE is found to be the factor of 128.

Table 6: Comparison of the efficiency for cavity-dose calculations by the implementation of photon cross-section enhancement technique using EGSnrc Monte Carlo user code for various ion chamber geometries

Type of simulation	NRC 3C ion chamber (cylindrical)				Pancake ion chamber (parallel-plate)				Farmer-type ion chamber							
									NE2571				N30013			
	Cavity dose (Gy)	σ	ϵ	CPU time (s)	Cavity dose (Gy)	σ	ϵ	CPU time (s)	Cavity dose (Gy)	σ	ϵ	CPU time (s)	Cavity dose (Gy)	σ	ϵ	CPU time (s)
XCSE factor																
-	1.20e-12	± 5.65	18	6.3	5.33e-12	± 3.01	12	35.2	3.10e-08	± 0.36	222	121	3.11e-08	± 0.169	603	210
2	1.26e-12	± 2.22	12	46.3	5.506e-12	± 0.8	10	510.5	3.294e-08	± 0.212	114	699	3.6034e-08	± 0.031	203	1844
4	1.23e-12	± 1.78	21	54	5.514e-12	± 0.5	16	648.5	3.303e-08	± 0.151	118	1327	3.6035e-08	± 0.023	366	1859
8	1.22e-12	± 1.26	32	70.4	5.507e-12	± 0.4	22	917.4	3.301e-08	± 0.109	117	2573	3.6037e-08	± 0.022	399	1860
16	1.25e-12	± 0.91	42	102.9	5.508e-12	± 0.3	27	1472	3.297e-08	± 0.079	113	5089	3.6040e-08	± 0.017	660	1886
32	1.22e-12	± 0.66	49	167.3	5.503e-12	± 0.2	35	2547	3.297e-08	± 0.056	128	8945	3.6038e-08	± 0.017	643	1937
64	1.23e-12	± 0.60	50	199.4	5.506e-12	± 0.15	43.3	3692	3.298e-08	± 0.046	183	9278	3.6036e-08	± 0.017	640	1946
128	1.23e-12	± 0.48	52	297.5	5.508e-12	± 0.1	76	4699	3.299e-08	± 0.031	371	10083	3.6034e-08	± 0.016	699	2012
256	1.24e-12	± 0.35	50	555.3	5.508e-12	± 0.1	40.1	8975	3.302e-08	± 0.025	286	20080	3.6046e-08	± 0.023	312	2188
512	1.23e-12	± 0.27	44	1077.9	5.507e-12	± 0.1	20.5	17482	3.325e-08	± 0.020	223	40216	3.3036e-08	± 0.031	147	2540

CPU: Computation, XCSE: Photon cross-section enhancement, NRC: National research council

Efficiency gain by the implementation of photon cross-section enhancement and range-rejection-based Russian roulette

In this part of the work, the method of XCSE technique has been adopted. The investigation focuses on the effect of range-rejection-based RR techniques using EGSnrc MC `egs_chamber` user code to carry out the objective of the present work. In Table 7, the type of simulation, quantity of interest (i.e., the cavity dose), relative statistical uncertainty σ , and simulation efficiency ϵ are depicted. Table 7 summarizes the effects of the combination of XCSE and range-rejection-based RR technique. The results clearly depict that when the XCSE factor is enhanced, similar levels of cavity doses occur, along with significant decreases in the relative statistical uncertainty from $\pm 5.65\%$ to $\pm 0.27\%$ for NRC 3C cylindrical ion chamber, $\pm 3.01\%$ to $\pm 0.076\%$ for parallel-plate pancake ion chamber, and $\pm 0.36\%$ to $\pm 0.3\%$ for NE2571 whereas it gets increased by 0.1% for N30013-modeled Farmer-type ion chambers without compromising accuracy. Table 7 shows the efficiency gained by the simulation using the combination of XCSE and range-rejection-based RR technique. The efficiency of the simulation is increased significantly up to a factor >260 for NRC 3C cylindrical ion chamber, 374 for parallel-plate pancake ion chamber, 430 and 978 for NE2571 and N30013-modeled Farmer-type ion chambers when compared to the simulation without using the VRT. When combining the effect of XCSE and range-rejection-based RR, it is quite possible to improve significantly the simulation efficiency.

It is clearly shown from sections of “Efficiency gain by range-rejection-based RR” and “efficiency gain by implementing XCSE” that the range-rejection-based RR focuses only on nonfat electrons and that fat electrons are being excluded from the XCSE technique. Hence, when ultimately implementing the effect of the combination of these

two methods in an appropriate way, the simulation efficiency will be improved. The efficiency is reduced, however, when enhancing the XCSE factor >128 . As it is clearly shown from the agreement between the previous section and this section, the optimized value of XCSE factor is found to be the factor of 128.

Comparison of computation time and efficiency of the simulation using all combinations of variance reduction techniques

In this section, the gain of computation time and simulation efficiency is compared for various combinations of VRTs that have been dealt in the preceding five sections. Figure 1a-d shows the computation times for the simulation of various ion-chamber dose calculations, using EGSnrc user codes such as `cavity` and `egs_chamber`, as a function of several combinations of VRTs obtained for 6 MV photon beams for Farmer-type (NE2571 and N30013) ionization chambers and 1.25 MeV ^{60}Co photon beams for cylindrical type (NRC and pancake) ionization chamber. Figure 1a-d shows that the computation time for RR technique is small, when compared to other individual and combinations of VRTs, since the computation time is not wasted on following the nonrelevant events involved in the interaction. Based on the explanations of results, it is concluded that the following order offers the best gain of computation time for simulations:

$$(RR) < (PS + RR) < (XCSE + RR) < (PS) < (XCSE)$$

Figure 2a-d depicts the comparisons of efficiency of simulations between various combinations of VRTs obtained for 6 MV photon beams for Farmer-type (NE2571 and N30013) ionization chambers and 1.25 MeV ^{60}Co photon beams for cylindrical type (NRC and pancake) ionization chamber. The graph shows that a very significant gain of efficiency has been achieved when implementing the combination of XCSE and

Table 7: Comparison of the efficiency for cavity-dose calculations by the implementation of photon cross-section enhancement+Russian roulette technique using EGSnrc Monte Carlo user code for various ion chamber geometries

Type of simulation	NRC 3C ion chamber (cylindrical)				Pancake ion chamber (parallel-plate)				Farmer-type ion chamber										
	Cavity dose (Gy)	σ	ϵ	CPU time (s)	Cavity dose (Gy)	σ	ϵ	CPU time (s)	NE2571				N30013						
									Cavity dose (Gy)	σ	ϵ	CPU time (s)	Cavity dose (Gy)	σ	ϵ	CPU time (s)			
XCSE + RR factor																			
-	1.20e-12	± 5.65	18	6.3	5.33e-12	± 3.01	12	35.2	3.10e-08	± 0.36	222	121	3.11e-08	± 0.169	603	210			
2	1.26e-12	± 2.22	12	46.3	5.506e-12	± 0.8	10	510.5	3.294e-08	± 0.212	114	699	3.6034e-08	± 0.031	203	1844			
4	1.23e-12	± 1.78	21	54	5.514e-12	± 0.5	16	648.5	3.303e-08	± 0.151	118	1327	3.6035e-08	± 0.023	366	1859			
8	1.22e-12	± 1.26	32	70.4	5.507e-12	± 0.4	22	917.4	3.301e-08	± 0.109	117	2573	3.6037e-08	± 0.022	399	1860			
16	1.25e-12	± 0.91	42	102.9	5.508e-12	± 0.3	27	1472	3.297e-08	± 0.079	113	5089	3.6040e-08	± 0.017	660	1886			
32	1.22e-12	± 0.66	49	167.3	5.503e-12	± 0.2	35	2547	3.297e-08	± 0.056	128	8945	3.6038e-08	± 0.017	643	1937			
64	1.23e-12	± 0.60	50	199.4	5.506e-12	± 0.15	43.3	3692	3.298e-08	± 0.046	183	9278	3.6036e-08	± 0.017	640	1946			
128	1.23e-12	± 0.48	52	297.5	5.508e-12	± 0.1	76	4699	3.299e-08	± 0.031	371	10083	3.6034e-08	± 0.016	699	2012			
256	1.24e-12	± 0.35	50	555.3	5.508e-12	± 0.1	40.1	8975	3.302e-08	± 0.025	286	20080	3.6046e-08	± 0.023	312	2188			
512	1.23e-12	± 0.27	44	1077.9	5.507e-12	± 0.1	20.5	17482	3.325e-08	± 0.020	223	40216	3.3036e-08	± 0.031	147	2540			

RR: Russian roulette, CPU: Computation, XCSE: Photon cross-section enhancement, NRC: National research council

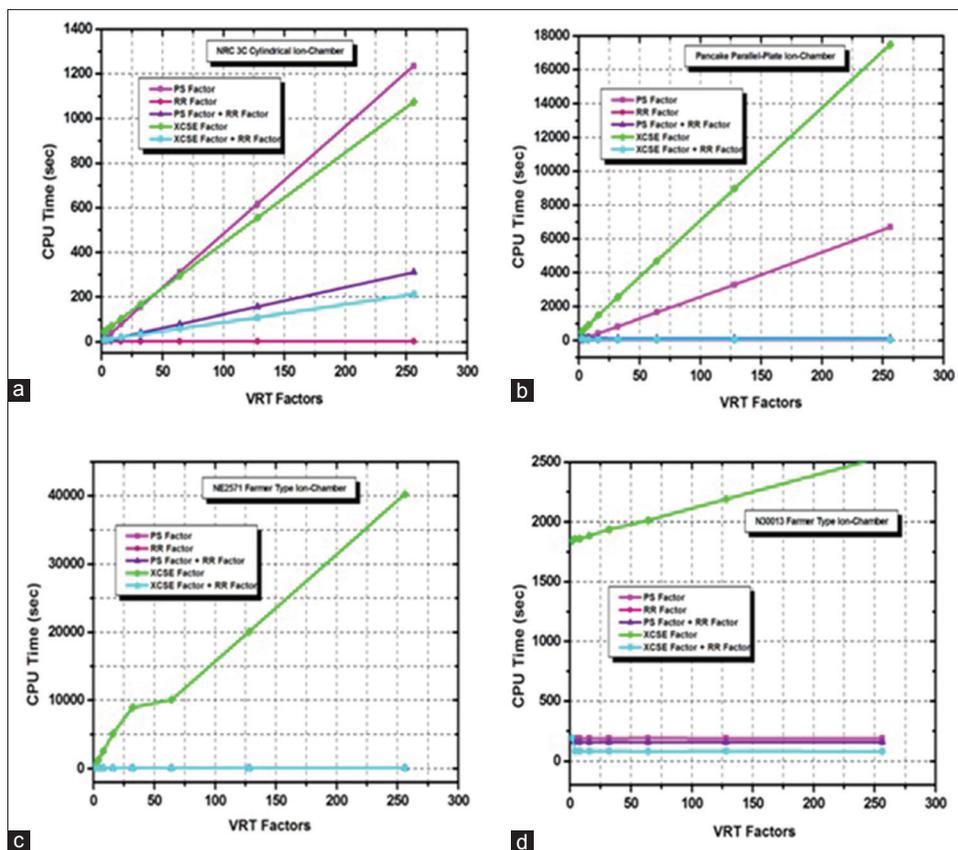


Figure 1: Computation time of various ion chamber dose calculations using EGSnrc Monte Carlo user codes as a function of several variance reduction technique factors; (a) NRC 3C ion chamber (b) parallel-plate pancake chamber (c) NE2571 Farmer-type ion chamber (d) N30013 Farmer-type ion chamber

RR for all cases. In this case, the efficiency is increased by a factor >260 for NRC 3C cylindrical ion chamber, 374 for parallel-plate pancake ion chamber, 430 and 978 for NE2571 and N30013 modeled Farmer-type ion chambers without affecting the accuracy of the simulation. This is due to the fact that these two combinations focus mainly on fat electrons so that the statistical weight of the particle is increased, which enhances the computation speed, thereby yielding the best efficiency.

From the above explanation, the result emerges that the following order offers the best gain of efficiency: (XCSE + RR) > (PS + RR) > (XCSE) > (RR) > (PS)

Hence, it is concluded that a proper combination of VRTs will significantly improve the efficiency of calculations and will substantially increase the computation speed.

BEAMnrc validation

After evaluating the VRTs, the validation of BEAMnrc MC simulation code has been carried out by employing the appropriate combination of VRTs. In general, BEAMnrc user code of EGSnrc MC Code^[12,15] is used to model the treatment head of the linear accelerator. It creates a phase space file which will then be used as a source for DOSXYZnrc user code to calculate the dose distributions in three-dimensional images. In this validation part, we have reconciled the component

module of N30013 ion chamber to be a water phantom with a cylindrical geometry of 25 cm radius. The central axis of this phantom was divided into voxels with equal dimensions of 0.5 cm in all directions. The dose has been calculated in these voxels using DOSXYZnrc MC User code.

To validate our model, the relative percentage depth dose calculations for reference field size (10 cm × 10 cm) by normalizing the dose at 10 cm depth and were compared with the experimental values which are shown in Figure 3a. Further, we used the local dose differences concept for an effective comparison of simulated values with the experimental values which are illustrated in Figure 3b. Table 8 depicts the comparison between our results obtained by BEAMnrc (with appropriate VRT’s combination) and BEAMnrc (without VRT). From the table, it has been clearly pointed out that the BEAMnrc with VRTs explicit a speed and accurate calculation with an acceptable uncertainty limit of 0.176% when compared to BEAMnrc without VRTs. Further, the efficiency of the simulation also has been increased by a factor of 195 for BEAMnrc MC Simulation of linac with VRTs when compared to the simulation without using the VRTs.

Based on the above results, it has been concluded that, for accurate dose calculations with minimal uncertainty and computation time, BEAMnrc MC Simulation employed with

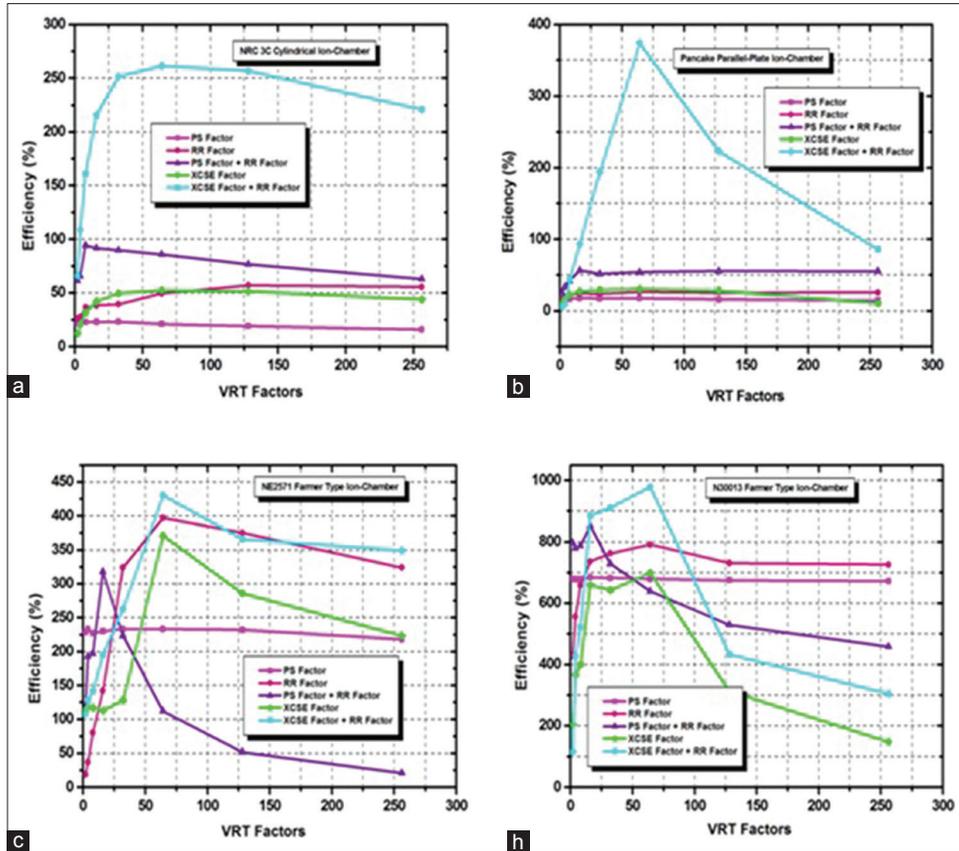


Figure 2: Efficiency of various ion chamber dose calculations using EGSnrc Monte Carlo user codes as a function of several variance reduction technique factors; (a) NRC 3C ion chamber (b) Parallel-plate pancake chamber (c) NE2571 Farmer-type ion chamber (d) N30013 Farmer-type ion chamber

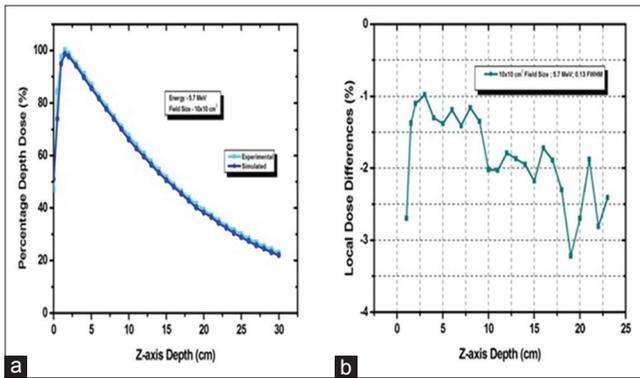


Figure 3: (a) Comparison of BEAMnrc Monte Carlo simulated and measured percentage depth dose curves of 10 cm x 10 cm field size for 6 MV photon beams. (b) The local dose differences

VRTs are found to be the most appropriate treatment planning method in the field of teletherapy.

CONCLUSION

MC simulation is an important tool in the field of modern radiotherapy. The EGSnrc MC code that simulates the radiation transport of coupled electron-gamma transport over a wide energy range has a library of VRTs. In this work, a few combinations of promising VRTs have been tested

Table 8: Comparison of the efficiency and computation time for cavity-dose calculations by the implementation of with and without variance reduction techniques using BEAMnrc Monte Carlo user code for 6 MV Varian linac

Type of simulation	Number of histories	σ	ϵ	CPU time (s)
BEAMnrc (with VRTs)	1×10^8	± 0.17	195	625
BEAMnrc (without VRTs)	1×10^8	± 1.36	0.15	3877.4

VRTs: Variance reduction techniques, CPU: Computation

with the intention of improving the simulation efficiency. The proper combination of these VRTs can yield significant improvement in the efficiency of the simulation of ion-chamber dose calculations. Our work demonstrated that the efficiency of the simulation is increased by a factor >260 for NRC 3C cylindrical ion chamber, 374 for parallel-plate pancake ion chamber, 430 and 978 for NE2571 and N30013-modeled Farmer-type ion chambers, along with a substantial step-down in the computation time when implementing the combination of XCSE and RR when compared to other VRTs.

Further, the evaluated VRTs were applied to validate BEAMnrc MC Simulation code through relative beam characteristics. A good agreement has been achieved between the simulated and experimental values for percentage depth dose curves

with a local difference of <3%. It has been observed that the BEAMnrc simulation with VRT yields higher efficiency and fast computation time with minimal uncertainty when comparing simulation without VRT. Hence, from this chapter, it is concluded that the BEAMnrc MC simulation with VRTs possess accurate dose calculations in the field of teletherapy apart from linac modeling.

Acknowledgment

One of the authors (Dr. C. S. Sureka) would like to acknowledge the “International Centre for Theoretical Physics (ICTP), Trieste, Italy,” for provided training to understand the basics of the EGSnrc MC code.

Financial support and sponsorship

Nil.

Conflicts of interest

There are no conflicts of interest.

REFERENCES

- Chan K, Heng SM, Smee R. Applications of Monte Carlo Methods in Biology, Medicine and Other Fields of Science. In: Mode CJ, editor. Application of Monte Carlo Simulation in Treatment Planning for Radiation Oncology. Published under CC BY-NC-SA 3.0 License. INTECH, 147-154, Academic Press; 2011.
- Prahl SA, Keijzer M, Jacques SL, Welch AJ. A Monte Carlo Model of Light Propagation in Tissue. SPIE Institute Series Vol. 5; 1989.
- Garcia-Pareja S, Vilches M, Lallena AM. Ant colony method to control variance reduction techniques in the Monte Carlo simulation of clinical electron linear accelerators. Nucl Instrum Methods Phys Res A 2007;580:510-3.
- Rodriguez M, Sempau J, Brualla L. A combined approach of variance-reduction techniques for the efficient Monte Carlo simulation of linacs. Phys Med Biol 2012;57:3013-24.
- Wulff J, Zink K, Kawrakow I. Efficiency improvements for ion chamber calculations in high energy photon beams. Med Phys 2008;35:1328-36.
- Seuntjens J, Beaulieu L, El Naqa I, Després P. Special section: Selected papers from the fourth international workshop on recent advances in Monte Carlo techniques for radiation therapy. Phys Med Biol 2012;57:57.
- De Marco JJ, Chetty IJ, Solberg TD. A Monte Carlo tutorial and the application for radiotherapy treatment planning. Med Dosimetry 2002;27:43-50.
- Hayati H, Mesbahi A, Nazarpour M. Monte Carlo modeling of a conventional X-ray computed tomography scanner for gel dosimetry purposes. Radiol Phys Technol 2016;9:37-43.
- Rogers DW, Bielajew AF. Monte Carlo techniques of electron and photon transport for radiation dosimetry. In: Kase KR, Bjarngard BE, Attix FH, editors. The Dosimetry of Ionizing Radiation. Vol. 3, Ch. 5. INTECH, 147-154. Academic Press; 2010.
- Eckhardt R. Stan Ulam, John Von Neumann and the Monte Carlo method. Los Alamos Sci 1987;15:1-137.
- Ulam S, Richtmyer RD, Von Neumann J. Statistical methods in neutron diffusion. Los Alamos Scientific Laboratory Report LAMS-551; 1947.
- Kawrakow E, Mainegra-Hing DW, Rogers FT, Walters BR. The EGSnrc Code System: Monte Carlo Simulation of Electron and Photon Transport. NRCC Report PIRS-701; 2011.
- Kawrakow I, Fippel M. Investigation of variance reduction techniques for Monte Carlo photon dose calculation using XVMC. Phys Med Biol 2000;45:2163-83.
- Rogers DW, Kawrakow I, Seuntjens JP, Walters BR, Mainegra-Hing E. NRC User Codes for EGSnrc. NRCC Report No. PIRS-702 (rev B). National Research Council of Canada; 2006.
- Kawrakow I. Lecture 17 Variance Reduction Techniques-IAEA Workshop on Monte Carlo. Trieste, Italy: International Center for Theoretical Physics; October, 2011. p. 17-28.
- Haugh M. Monte Carlo Simulation: IEOE E4703. Simulation Efficiency and an Introduction to Variance Reduction Methods. INTECH, 147-154. Academic Press; 2010.
- Atzberger PJ. Strategies for Improving the Efficiency of Monte Carlo Methods, Semantic scholar 2006.
- Walters BR. Increasing efficiency of BEAMnrc-simulated co-60 beams using directional source biasing. Med Phys 2015;42:5817-27.
- Mora GM, Maio A, Rogers DW. Monte Carlo simulation of a typical 60Co therapy source. Med Phys 1999;26:2494-502.
- Sweezy J, Brown F, Booth T, Chiamonte J, Preeg B. Automated variance reduction for MCNP using deterministic methods. Radiat Prot Dosimetry 2005;116:508-12.
- Kawrakow I. On the efficiency of photon beam treatment head simulations. Med. Phys 1995;22:503-24.
- Ono T, Araki F, Yoshiyama F. Perturbation correction factors for cylindrical ionization chambers in high energy electron beams. Radiol Phys Technol 2010;3:93-97.
- C. Arun, T. Palaniselvam, Verma Dinkar, Prabhat Munshi, Manjit Singh Kalra. Monte Carlo- based energy studies of diode dosimeters in radiotherapy beams. Radiol Phys Technol. 2013;6:151-6.
- G. Gualdrini and Ferrari. Monte Carlo Variance reduction techniques: An overview with some practical examples. Rad. Pro Dos 146:4:425-33.
- Rogers DW, Kawrakow I, Seuntjens JP, Walters BR, Mainegra-Hing E. “NRC user code for EGSnrc.” NRCC report PIRS-702 (rev C) 2011.